

Rapid Radio Flaring during an Anomalous Outburst of SS Cyg

K. P. Mooley^{1,9}, J. C. A. Miller-Jones², R. P. Fender¹, G. R. Sivakoff³, C. Rumsey⁴,
 Y. Perrott⁴, D. Titterington⁴, K. Grainge⁵, T. D. Russell^{2,6}, S. H. Carey⁴, J. Hickish⁴,
 N. Razavi-Ghods⁴, A. Scaife⁵, P. Scott⁴, E. O. Waagen⁷

¹ Centre for Astrophysical Surveys, University of Oxford, Denys Wilkinson Building, Keble Road, Oxford OX1 3RH

² International Centre for Radio Astronomy Research - Curtin University, GPO Box U1987, Perth, WA 6845, Australia

³ Department of Physics, University of Alberta, 4-181 CCIS, Edmonton, AB T6G 2E1, Canada

⁴ Astrophysics Group, Cavendish Laboratory, 19 J. J. Thomson Avenue, Cambridge CB3 0HE, UK

⁵ University of Manchester, Alan Turing Building, Oxford Road, Manchester M13 9PL, UK

⁶ Anton Pannekoek Institute for Astronomy, University of Amsterdam, PO Box 94249, NL-1090 GE Amsterdam, Netherlands

⁷ American Association of Variable Star Observers, 49 Bay State Road, Cambridge, MA 02138, USA

⁹ Hintze Research Fellow; Email: kunal.mooley@physics.ox.ac.uk

23 November 2016

ABSTRACT

The connection between accretion and jet production in accreting white dwarf binary systems, especially dwarf novae, is not well understood. Radio wavelengths provide key insights into the mechanisms responsible for accelerating electrons, including jets and outflows. Here we present densely-sampled radio coverage, obtained with the Arcminute MicroKelvin Imager Large Array, of the dwarf nova SS Cyg during its February 2016 anomalous outburst. The outburst displayed a slower rise (3 days mag⁻¹) in the optical than typical ones, and lasted for more than 3 weeks. Rapid radio flaring on timescales <1 hour was seen throughout the outburst. The most intriguing behavior in the radio was towards the end of the outburst where a fast, luminous (“giant”), flare peaking at ~20 mJy and lasting for 15 minutes was observed. This is the first time that such a flare has been observed in SS Cyg, and insufficient coverage could explain its non-detection in previous outbursts. These data, together with past radio observations, are consistent with synchrotron emission from plasma ejection events as being the origin of the radio flares. However, the production of the giant flare during the declining accretion rate phase remains unexplained within the standard accretion-jet framework and appears to be markedly different to similar patterns of behavior in X-ray binaries.

Key words: radio continuum: stars — X-rays: stars — stars: dwarf novae

1 INTRODUCTION

Dwarf novae (DNe) are binary systems containing a non-magnetic ($B_{\text{surface}} < 10^6$ G) white dwarf actively accreting from a Roche lobe-filling main-sequence companion via an accretion disk (Warner 1995). All known DNe undergo episodic outbursts, which last between a few days and a few years, recur between 10 days and several decades, and result in brightening by 2–8 magnitudes in the optical (e.g. Coppejans et al. 2016a). The disk instability model, in which the accretion disk cycles between cool quiescent states and hot outburst states, provides a consistent framework for explaining these outbursts (e.g. Osaki 1974; Meyer & Meyer-Hofmeister 1981; Lasota 2001). DN outbursts seem to be analogous to X-ray binary (XRB) outbursts (e.g. Kuulkers, Howell & van Paradijs 1996), and the similarities between their hardness-intensity diagrams (disk-fraction luminosity diagram, or DFLD, in the case of DNe) together with the presence of transient radio emission suggests that the connection between the outburst phase and the radio (jet) emission could be similar as well (Körding et al. 2008).

While some classes of accreting white dwarf systems, such as symbiotic stars, and magnetic cataclysmic variables, were detected in the radio¹, DNe were, until recently, thought to be weak radio emitters (e.g. Soker & Lasota 2004). Even for the few DNe that were detected in the radio during outbursts, the detection was not reproducible (e.g. Benz, Fuerst & Kiplinger 1983; Benz, Güdel & Mattei 1996). Coppejans et al. (2015) and Coppejans et al. (2016b) showed that many of the non-magnetic accreting white dwarf systems are faint ($\lesssim 0.1$ mJy) and variable on ~hours timescales in the radio, and that the sensitivities, time-resolutions or timing of previous observations were insufficient to detect these fainter systems. DNe have now been shown to be repeating radio emitters during outbursts (Coppejans et al. 2016b; Russell et al. 2016). The brightness temperature from VLBI imaging, the out-

¹ Radio emission is also expected from supersoft X-ray sources, which show evidence for jets through pairs of Doppler shifted emission lines.

burst track in the DFLD, the radio spectral indices, and the shape of the radio light curves have been used to argue in support of synchrotron emission from a transient jet as the cause of the radio emission during DNe outbursts (Körding et al. 2008; Russell et al. 2016; Coppejans et al. 2016b).

The quintessential DN, SS Cyg, is one of the best studied systems of its class across the electromagnetic spectrum. This system consists of a $\sim 1 M_{\odot}$ white dwarf with a K5V companion, with the inclination of the binary being close to 45° (North et al. 2002; Körding et al. 2008). The precise VLBI parallax distance measurement² of 114 ± 2 pc (Miller-Jones et al. 2013) allows the study of the energetics of this system at a level of precision impossible to achieve for most accreting systems. Long-term optical monitoring of SS Cyg has revealed regular outbursts lasting ~ 5 –20 days and recurring on timescales between ~ 20 –60 days (Cannizzo & Mattei 1992). The majority of the outbursts have rise and decay rates (in the optical) that are remarkably similar from one outburst to another, and scattered around $0.5 \text{ days mag}^{-1}$ and $2.5 \text{ days mag}^{-1}$ respectively. About 10% of the outbursts, referred to as “anomalous”, exhibit a slow rise of $\gtrsim 1.5 \text{ days mag}^{-1}$ in the optical (Cannizzo & Mattei 1998). X-ray and ultraviolet observations suggest that accretion in SS Cyg (and similarly in other dwarf novae) occurs via a “boundary region” between the inner accretion disk and the surface of the white dwarf. The boundary region becomes optically thick at X-ray frequencies at the onset of an outburst and may play a role in jet production in SS Cyg (Wheatley et al. 2003; Russell et al. 2016). Analogous to XRBs, SS Cyg is expected to have a steady jet during the rise phase of an outburst and discrete plasma ejection after the subsequent spectral softening (Körding et al. 2008; Miller-Jones et al. 2011).

In February 2016, SS Cyg underwent an anomalous outburst, which lasted for about 3 weeks (at $V > 11$ mag). The outburst showed a slow rise of about 3 days mag^{-1} in the optical for one week and then transformed into a standard broad outburst before reaching the peak. Here, we report on high-cadence radio observations of this anomalous outburst of SS Cyg. In §2 we describe the optical, radio and X-ray observations, and present our analysis and discussion in §3.

2 OBSERVATIONS AND DATA PROCESSING

2.1 Optical

We requested close monitoring of SS Cyg and immediate submission of observations to the American Association of Variable Star Observers (AAVSO; Special Notice #412, Alert Notice 536) in order to catch the rise phase of the outburst and obtain a well-sampled optical light curve. Good sampling at the beginning of the outburst was necessary for triggering the radio observations (see below). The data were downloaded from the AAVSO website³. We used the V band magnitudes for our analysis. The optical light curve is shown in Figure 1.

2.2 Radio

We monitored the AAVSO light curve, and once the optical light curve reached 11.5 mag in the pre-validated V band (on 2016 Feb 11), we triggered the Arcminute MicroKelvin Imager Large Array (AMI-LA; Zwart et al. 2008) radio telescope. Observations were made with the new digital correlator having 4096 channels across

a 5 GHz bandwidth between 13–18 GHz. SS Cyg was monitored for about 10 hours every day throughout the ~ 3 weeks of outburst. The phase calibrator, J2153+4322, was observed every 12 minutes for about 1.5 minutes. The log of AMI-LA observations is given in Table 1.

The AMI-LA data were binned to 8×0.625 GHz channels and processed (RFI excision and calibration) with a fully-automated pipeline, AMI-REDUCE (e.g. Davies et al. 2009; Perrott et al. 2013). Daily measurements of 3C48 and 3C286 were used for the absolute flux calibration, which is good to about 10%. The calibrated amplitudes for J2153+4322 showed variability of 20% (peak-to-peak) around the mean of 250 mJy at 15.5 GHz within each 10-hour observing block. This variability in the complex gain calibrator is likely a combination of unmodeled gain variations and pointing errors⁴. Hence we recalibrated the data using fixed values for the flux density ($S_{15.5\text{GHz}} = 260$ mJy) and spectral index ($\alpha = -0.15$; $S \propto \nu^{\alpha}$) of J2153+4322, which are our best estimates based on our knowledge of the instrument and the data. Conservative uncertainties in these estimates are 5% (flux density) and 0.1 (spectral index), and hence we conclude that the error in flux density is dominated by the absolute flux scale uncertainty. While there are no published 15 GHz flux density measurements for J2153+4322, the flux density and the spectral index that we have used are consistent with its 8.4 GHz flux densities measured in 2011⁵.

The calibrated and RFI-flagged data were then imported into CASA. Since the AMI-LA synthesized beam is approximately $30''$, the ~ 1 mJy radio source $22.3''$ to the North-West of SS Cyg causes confusion and had to be subtracted from the UV plane. We used the interactive mode of CASA `clean` to define a restricted clean box at the coordinates of the confusing source (the clean box does not overlap with the location of SS Cyg) and derived a model for each AMI-LA observation. We then loaded and subtracted the model from the CASA measurement sets using the tasks `ft` and `uvsub`. We then split each 10-hour observation into shorter intervals as needed, according to the variability seen in the source, and imaged each interval using CASA `clean`. The flux density of SS Cyg was measured in the resulting $512 \times 512 \text{ pix}^2$ ($4'' \text{ pix}^{-1}$) images using the `pyfits` module.

The AMI-LA light curve is shown in Figure 1. We present a discussion of it in §3.

2.3 X-ray

A 1 ks Swift XRT observation⁶ was carried out on 2016 Feb 18.136 (start time; MJD 57436.136). In 971.7 s of data, we detect a count rate of 1.887 ± 0.049 per second in the 0.3–10 keV band. The X-ray observation was not strictly simultaneous with any optical or radio observations.

A multi-temperature plasma emission model is often used to describe the X-ray spectra of dwarf novae, in which the boundary layer is heated to $\sim 10^8$ K during outburst (e.g. Wheatley et al. 2003; Pandel et al. 2005). Accordingly, we fit a `cemekl` model (the emission measures in this model follow a power law in temperature up to a certain maximum; Done & Osborne 1997) to the binned XRT spectrum using `XSpec` and obtained a maximum temperature

⁴ We note, however, that significant work has gone into improving the AMI-LA amplitude gain calibration and empirical pointing model.

⁵ ~ 280 mJy from <http://astrogeo.org/v2m/maps/bc196zc/> and Russell et al. (2016), for example

⁶ Some of the requested XRT observations were interrupted by GRB observations.

² The Gaia distance is 117 ± 4 pc (Gaia Collaboration 2016).

³ <https://www.aavso.org/data-download>

of $19.6_{-4.3}^{+7.0}$ keV. In the 0.5–10 keV, 1–10 keV, and 2–10 keV bands, this model has a flux of 6.5, 5.5, and $4.3 (\times 10^{11})$ erg s⁻¹ cm⁻² respectively. At a distance of 114 pc, we get a luminosity of $L_X = 1.7 \times 10^{31}$ erg s⁻¹ in the 1–10 keV band.

3 RESULTS & DISCUSSION

Our AMI-LA observations of SS Cyg during the February 2016 anomalous outburst represent the most densely-sampled radio coverage of any dwarf nova thus far. The radio light curve at 15.5 GHz is shown in Figure 1 along with the optical light curve. Our radio coverage began as soon as the optical light curve reached $V = 11$ mag. (on 11 February 2016), and we find evidence for radio emission from SS Cyg right from our first observation, at a 15.5 GHz flux density of 57 ± 17 μ Jy. Our previous AMI-LA observation from 02 February gave a non-detection, with a 2σ upper limit⁷ of 86 μ Jy. We do not detect any significant intra-day and inter-day variability in the observations carried out between 11–13 February (MJD 57429–57431).

We detected significant variability on \sim hour timescales starting on 14 February. A comparison with a “normal” optical outburst (grey points in Figure 1) suggests that the flaring started when the normal optical outburst would have been expected to begin. Further observations are necessary to verify whether this is indeed the case during a normal optical outburst. The first flare occurred towards the end of our AMI-LA observation carried out on 14 February (MJD 57432.6726), at a peak flux density of 204 ± 34 μ Jy at 15.5 GHz. Subsequently, a series of rapid flares, with rise times between 5–30 minutes were seen throughout the outburst. While the majority of the radio flares peaked at sub-mJy flux densities, we detected a very luminous flare towards the end of the outburst, peaking at 18.0 ± 0.4 mJy at 15.5 GHz and lasting for only \sim 15 minutes. The radio light curves at 14.25 GHz and 16.75 GHz⁸ for this fast luminous flare (“giant” flare) are shown in Figure 2. There is some evidence of radio brightening of SS Cyg towards the end of the April 2007 and April 2016 outbursts as well (Körding et al. in prep, Miller-Jones et al. in prep), which may suggest the presence of such a giant flare is a common feature of outbursts in SS Cyg. If so, then such a flare could have been missed in the majority of the past radio observations (those reported by Russell et al. 2016) due to their much sparser time coverage. Overall, during the outburst, the radio emission lasted for 3 weeks (11 February to 02 March 2016, i.e. MJD 57432–57449; above our 2σ detection threshold of \sim 40 μ Jy).

The initial radio flares, seen over a span of \sim 1 week (between MJD 57432 and 57439), had rise times of tens of minutes and at peak they had an optically thick spectrum at 15.5 GHz. Each successive flare was seen to have a peak flux density higher than the previous one. If this flaring activity is related to plasma ejection events, then the optically thick spectrum (with $0 \lesssim \alpha_{14.2\text{GHz}}^{16.8\text{GHz}} \lesssim 2$) suggests that the particle acceleration time is shorter than the expansion timescale of the ejected blobs. This initial set of flares, which continued into the peak/flattening of the optical light curve, was followed by a few days where the radio emission was fairly

steady or rising gradually. The 15.5 GHz flux density was between 100–200 μ Jy during this phase. This steady period may be related to the “plateau” phase seen during past radio observations of SS Cyg (e.g. Körding et al. 2008; Russell et al. 2016), although the coverage of these previous observations was very sparse. Between MJD 57443 and 57446, the flaring activity resumed and during this period the overall spectrum at the flare peak was optically thinner than the earlier flares. In general, the flare peaks are short lived and hard to define, but probably represent optically thick to thin transition⁹. The multiple radio flares seen throughout the outburst are unlikely to be caused by the source crossing the “jet line” multiple times, given the evolution in the DFLD (Körding et al. 2008), and may be either due to internal shocks, external shocks, or multiple discrete ejections not tied to any specific jet line.

In the first two hours of the AMI-LA observation on 29 February (MJD 57447.31), SS Cyg was at or below 150 μ Jy. On MJD 57447.4 we detected the onset of the giant flare (Figure 2). After a gradual increase in flux density to 1.5 mJy, the giant flare reached its peak in \sim 5 minutes (e-folding timescale of \sim 1.5 minutes). The implied variability brightness temperature is $T_B > 10^7$ K, which is comparable to or even greater than that seen in flares from magnetic CVs. This value can also be compared with the lower limits to the brightness temperature placed from VLBA observations, 5.4×10^6 K, and previously observed radio variability, 5.5×10^3 K (Russell et al. 2016). The T_B of the giant flare and other radio flares detected during the outburst is consistent either with a synchrotron origin of the flares, as noted by previous works (Körding et al. 2008; Russell et al. 2016), or with a coherent source of emission. Recently, 100% circularly polarized radio flares were detected in nova-like cataclysmic variables (Coppejans et al. 2015), indicating coherent emission. We can neither confirm nor rule out the coherent mechanism hypothesis through our radio observations since the AMI-LA does not provide any polarization information. The time resolution and sensitivity of the AMI-LA data are sufficient to (temporally) resolve the giant flare and get reliable spectral indices. During the rise phase of the giant flare, the spectral index ($\alpha_{14.2\text{GHz}}^{16.8\text{GHz}}$) is 0.8 ± 0.4 (MJD 57447.4042; $S_{15.5\text{GHz}} = 6.9 \pm 0.3$ mJy), which increases to 2.8 ± 0.3 (MJD 57447.4047; $S_{15.5\text{GHz}} = 10.5 \pm 0.4$ mJy), consistent with a fully self-absorbed synchrotron source. Beyond this maximum in the spectral index, the spectrum between 13–18 GHz evolves towards becoming optically thin. At the peak of the giant flare (MJD 57447.4064, $S_{15.5\text{GHz}} = 18.1 \pm 0.4$ mJy), the spectral index is 1.4 ± 0.2 , and then decreases to a minimum of -1.0 ± 0.2 (MJD 57447.4081; $S_{15.5\text{GHz}} = 13.7 \pm 0.4$ mJy) during the decay of the flare. At MJD 57447.4103, another mJy-level flare, optically thin and peaking at 3.9 ± 0.3 mJy at 16.75 GHz, is detected and may have a delayed, less-luminous, counterpart at 14.25 GHz at 57447.4125 (see Figure 2). Overall, the behavior of the radio emission at frequencies between 14.25 GHz and 16.75 GHz is consistent with the adiabatic expansion of a synchrotron-emitting plasma blob (van der Laan 1966).

The question of why there was a giant radio flare towards the end of the outburst warrants some consideration. According to the disk instability model¹⁰, the material accreted from the companion star gradually builds up in the accretion disk until the temperature

⁷ Although the convention is to quote 3σ upper limits, the known coordinates of SS Cyg together with our knowledge of the noise properties and the manual inspection of radio images allow us to confidently place the detection threshold at 2σ . <1 spurious detection is expected at this level.

⁸ Our flux density values at 15.5 GHz are the mean over the whole 13–18 GHz band, while the 14.25 GHz and 16.75 GHz measurements are means over the 13–15.5 GHz and 15.5–18 GHz bands.

⁹ Our default assumption, based on previous work (e.g. Russell et al. 2016), is that this is synchrotron emission, but we discuss the possibility of coherent emission in the context of the giant flare below.

¹⁰ Although the DIM cannot explain anomalous outbursts very well (Schreiber et al. 2003), the large flares occurs well after the slow-rise phase, once the outburst has apparently transitioned into a normal outburst.

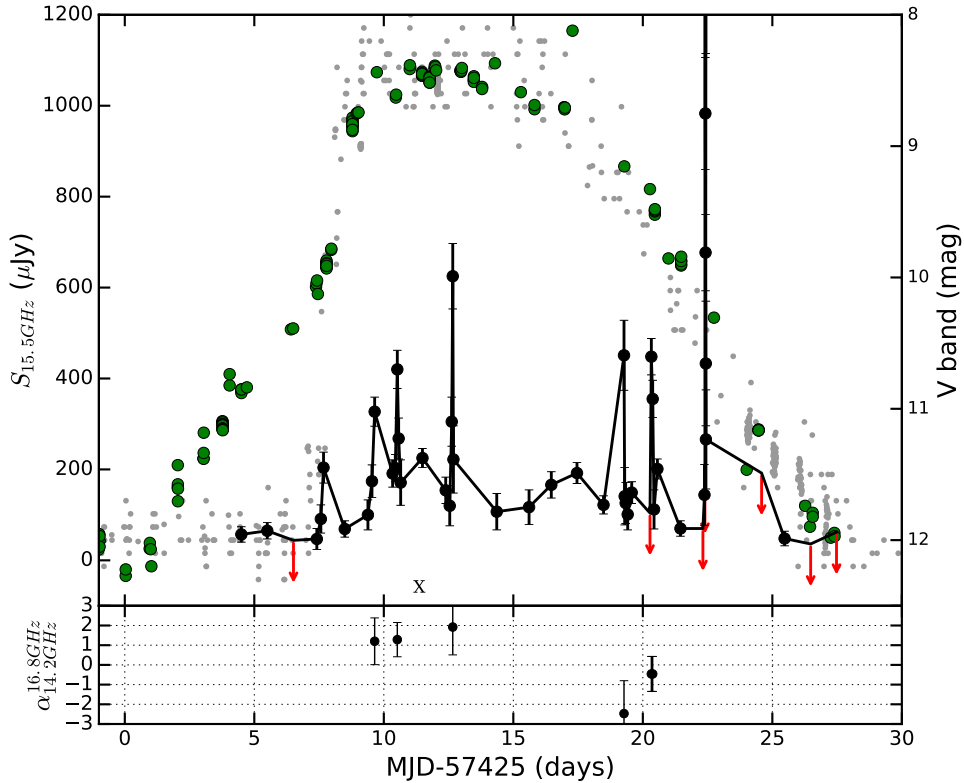


Figure 1. The 15.5 GHz AMI-LA (black) and V-band AAVSO (green) light curves of SS Cyg during the February 2016 anomalous outburst. Upper limits (2σ) in the radio are shown as red arrows. For comparison, the optical light curve for a normal outburst presented by K rding et al. (2008) is shown in grey (aligned at the steep rise). The “X” symbol denotes the time of the X-ray observation (see 2.3 for details). The “giant” flare peaking at ~ 18 mJy, seen on MJD 57447 (29 February 2016) and lasting for ~ 10 minutes, is shown in more detail in Figure 2. The upper limits on the day of the giant flare lie outside the time interval shown in Figure 2. Note that the peak of the giant flare extends much beyond the scale of this figure. The bottom panel shows the spectral indices ($S \propto \nu^\alpha$; between 14.25 GHz and 16.75 GHz) during peaks of flaring events seen at 15.5 GHz.

increases to the critical point to drive the hydrogen ionization instability, thereby transporting the accretion disk material rapidly onto the surface of the white dwarf. During outburst, the X-ray emission rises at a similar time as the optical, and this is attributed to the material reaching the boundary layer. The boundary layer becomes optically thick and quenches the X-ray radiation while the extreme UV radiation rises rapidly (Wheatley et al. 2003). Residual X-ray emission persists through the outburst phase. Our X-ray observation was carried out soon after the optical light curve reached peak (MJD 57436.14). The 1–10 keV luminosity, 1.7×10^{31} erg s $^{-1}$, is in agreement with past observations during this phase of the outburst. At the end of the optical and ultraviolet decay phases, the X-ray emission rises gradually, and later fades back to quiescent levels (Wheatley et al. 2003; Russell et al. 2016). During the phase when the optical and UV emission are declining, the accretion rate is expected to drop substantially. Hence the “giant” flare, seen towards the end of the outburst, is intriguing. If the giant flare is due to the ejection of plasma blob(s), then the large amplitude of the radio flare during this decay phase remains unexplained. A comparison between our observations and a normal optical outburst suggests that the giant flare occurs either slightly before or right at the start of the X-ray increase at the end of the outburst (see, e.g. Wheatley et al. 2003; Russell et al. 2016), 2–3 days before the peak of the X-ray emission. This suggests that the giant flare is not driven by the large change in the optical depth of the boundary layer. Although the magnetic field of the white dwarf in SS Cyg is not high, it is possible that something like the propeller effect or magnetic recon-

nection takes over as the accretion rate is falling and generates an outflow of gas (e.g. in cases of AE Aqr and VW Hyi; Wynn, King & Horne 1997; Warner & Woudt 2002; Meintjes & de Jager 2000), and hence a luminous flare in the radio. Since the isotropic 15.5 GHz luminosity at the peak of the giant flare (and $\alpha_{14.2\text{GHz}}^{16.8\text{GHz}} \simeq 1$) is $\sim 10^{27}$ erg s $^{-1}$, this flare may be consistent with the L_R to L_X relationship (using an estimate of the X-ray luminosity from Wheatley et al. 2003) seen for black hole systems (see figure 9 of Russell et al. 2016), albeit for a very short period of time.

Lastly, we would like to highlight the importance of densely-sampled radio coverage, without which the rapid flares and the giant radio flare (which had a duration of 15 minutes) towards the end of SS Cyg’s outburst would have remained unknown. The 200 hours of observing presented here may not be feasible with telescopes like the SKA or its pathfinders, and this underscores the need for interferometers like the AMI-LA to be operational in the era of large telescopes. Niche areas of astronomy will continue to be accessible only with such small radio interferometers.

Acknowledgements: KPM’s research is supported by the Oxford Centre for Astrophysical Surveys which is funded through the Hintze Family Charitable Foundation. JCAMJ is the recipient of an Australian Research Council Future Fellowship (FT140101082). RPF acknowledges support from the European Research Council Advanced Grant 267697 “4 Pi Sky: Extreme Astrophysics with Revolutionary Radio Telescopes”. TDR acknowledges support from the Netherlands Organisation for Scientific Research (NWO) Veni Fellowship, grant number 639.041.646. AMS gratefully acknowledges

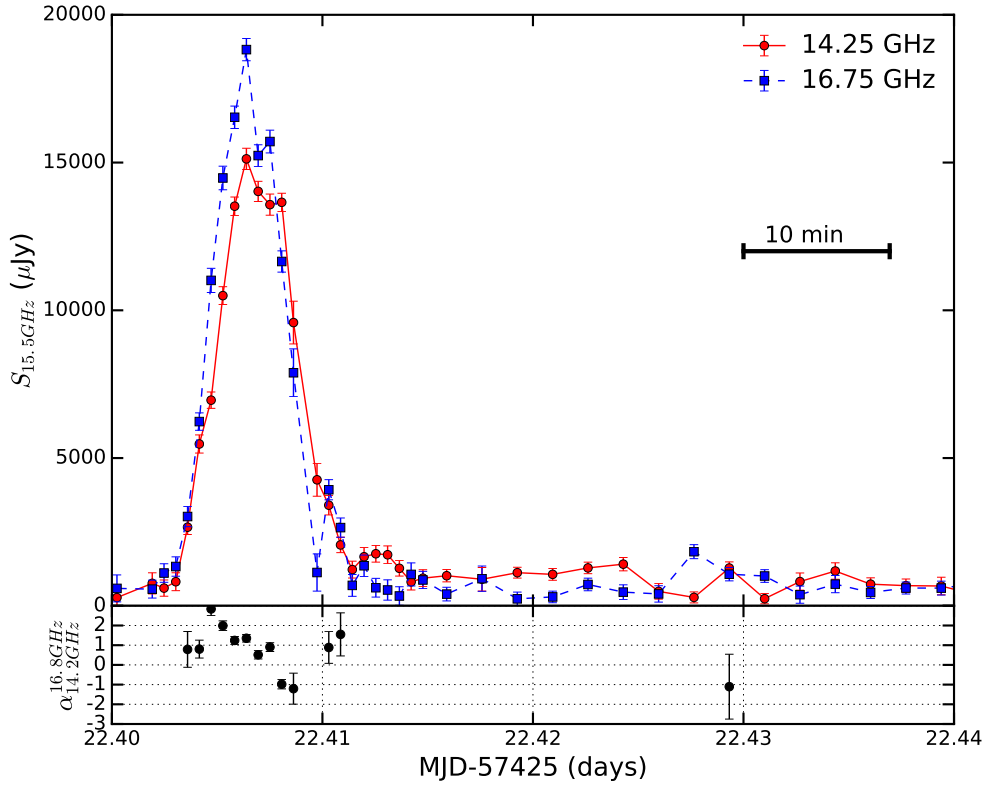


Figure 2. The radio light curves at 14.25 GHz and 16.75 GHz during the SS Cyg “giant” flare on MJD 57447 (29 February), using data from Table 2. The bottom panel shows the spectral indices between these two frequencies. None of the optical observations were strictly simultaneous with this flare.

support from the European Research Council under grant ERC-2012- StG-307215 LODESTONE. The AMI telescope is supported by the European Research Council under grant ERC-2012- StG-307215 LODESTONE, the UK Science and Technology Facilities Council (STFC) and the University of Cambridge. We extend special thanks to Stella Kafka for coordinating the optical observations on behalf of AAVSO, and to all the diligent AAVSO observers who contributed to the optical light curve. We thank the AMI and Swift staff for scheduling the radio and X-ray observations. We also thank the anonymous referee for providing useful comments.

REFERENCES

- Benz A. O., Fuerst E., Kiplinger A. L., 1983, *Nature*, 302, 45
 Benz, A. O., Güdel, M. & Mattei, J. A. 1996, *ASP Conference Series*, 93, 188
 Cannizzo, J. K. & Mattei, J. A. 1992, *ApJ*, 401, 642
 Cannizzo, J. K. & Mattei, J. A. 1998, *ApJ*, 505, 344
 Coppejans, D. L., Körding, E. G., Miller-Jones, J. C. A., Rupen, M. P., Knigge, C., et al. 2015, *MNRAS*, 451, 3801
 Coppejans, D. L., Körding, E. G., Knigge, C., Pretorius, M. L., Woudt, P. A., Groot, P. J., Van Eck, C. L. & Drake, A. J., 2016, *MNRAS*, 456, 4441
 Coppejans, D. L., Körding, E. G., Miller-Jones, J. C. A., Rupen, M. P., Sivakoff, G. R., Knigge, C., Groot, P. J., Woudt, P. A., Waagen, E. O. & Templeton, M. 2016, *MNRAS*, 463, 2229
 Davies, M. L. et al. 2009, *MNRAS* 400, 984
 Done, C. & Osborne, J. P., 1997, *MNRAS*, 288, 649
 Gaia Collaboration, A. G. A. Brown, A. Vallenari, T. Prusti, J. H. J. de Bruijne, F. Mignard et al. 2016, *A&A*, in press
 Körding, E., Rupen, M., Knigge, C., Fender, R., Dhawan, V., Templeton, M., & Muxlow, T. 2008, *Science*, 320, 1318
 Kuulkers, E., Howell, S. B., van Paradijs, J. 1996, *ApJ*, 462, 87
 Lasota, J.-P. 2001, *NAR*, 45, 449
 Meintjes, P. J. & de Jager, O. C. 2000, *MNRAS*, 311, 611
 Meyer, F. & Meyer-Hofmeister, E. 1981, *A&A*, 104, 10
 Miller-Jones, J. C. A., et al. 2011, in *IAU Symposium*, Vol. 275, ed. G. E. Romero, R. A. Sunyaev, & T. Belloni, 224
 Miller-Jones, J. C. A., Sivakoff, G. R., Knigge, C., Körding, E. G., Templeton, M. & Waagen, E. O. 2013, *Science*, 340, 950
 North, R. C., Marsh, T. R., Kolb, U., Dhillon, V. S., Moran, C. K. J. 2002, *MNRAS*, 337, 1215
 Osaki, Y. 1974, *PASJ*, 26, 429
 Pandel, D., Cordova, F. A., Mason, K. O. & Priedhorsky, W. C. 2005, *ApJ*, 626, 396
 Perrott, Y. C., Scaife, A. M. M., Green, D. A., Davies, M. L., Franzen, T. M. O. et al. 2013, *MNRAS*, 429, 3330
 Russell, T. D., Miller-Jones, J. C. A., Sivakoff, G. R., Altamirano, D., O’Brien, T. J., et al. 2016, *MNRAS*, 460, 3720
 Schreiber, M. R., Hameury, J. M., & Lasota, J. P. 2003, *A&A*, 410, 239
 Soker, N., & Lasota, J. P. 2004, *A&A*, 422, 1039
 van der Laan, H. 1966, *Nature*, 211, 1131
 Wheatley, P. J., Mauche, C. W., & Mattei, J. A. 2003, *MNRAS*, 345, 49
 Warner, B. 1995, *Cambridge Astrophysics Series*, 28
 Warner, B. & Woudt, P. 2002, *MNRAS*, 335, 84
 Wynn, G., King, A. & Horne, K. 1997, *MNRAS*, 286, 436
 Zwart, J. T. L., Barker, R. W., Biddulph, P., Bly, D., Boysen, R. C. et al. 2008, *MNRAS*, 391, 1545

Table 1. 15.5 GHz AMI-LA measurements of the SS Cyg

MJD	Dur. (min)	$S_{15.5GHz}$ (μ Jy)	σ_S (μ Jy)	$\alpha_{14.2GHz}^{16.8GHz}$	σ_α
57420.5991	117	81	43
57429.4993	598	57	17
57430.5007	598	65	18
57431.5124	596	41	22
57432.4136	298	47	23
57432.5690	149	90	31
57432.6726	149	204	34
57433.4925	598	69	18
57434.3865	299	100	33
57434.5423	149	174	36
57434.6462	149	327	32	1.2	1.2
57435.3398	149	191	30
57435.4434	149	203	30
57435.5210	74	420	42	1.3	0.9
57435.5728	74	268	45
57435.6505	149	171	50
57436.4919	596	225	21
57437.3896	298	154	29
57437.5449	149	120	44
57437.6226	74	305	54
57437.6615	37	625	72	1.9	1.4
57437.6874	37	222	74
57439.3601	239	107	40
57440.6077	317	117	38
57441.4665	598	166	29
57442.4577	580	192	23
57443.4824	596	122	20
57444.2729	37	451	77	-2.5	1.7
57444.2988	37	141	63
57444.3376	74	126	45
57444.4153	149	101	34
57444.5707	298	149	24
57445.2764	74	89	52
57445.3284	74	448	40	-0.5	0.9
57445.3803	74	355	41	-0.5	0.9
57445.4323	74	112	43
57445.5621	299	201	22
57446.4529	598	70	17
57447.3196	137	47	35
57447.3793	34	147	67
57447.3972	17	88	76
57447.4046	4	9254	175
57447.4076	4	15845	184
57447.4106	4	2843	149
57447.4136	4	983	123
57447.4210	17	677	84
57447.4285	4	1239	124
57447.4315	4	433	137
57447.4359	8	249	109
57449.5854	266	91	96
57450.4727	595	52	16
57451.4792	536	2	18
57452.4772	596	10	31

Notes: a) $S_{15.5GHz}$ is the peak pixel values at the location of SS Cyg. Flux density values that are $<2\sigma$ are to be considered as non-detections. b) σ_S is the RMS noise. c) The spectral index values have large uncertainties except in the cases of flare peaks, and only those values are noted here.

Table 2. 15.5 GHz finely sampled measurements of the “giant” flare

MJD	Dur. (min)	$S_{15.5GHz}$ (μ Jy)	σ_S (μ Jy)	$\alpha_{14.2GHz}^{16.8GHz}$	σ_α
57447.39745	0.8	547	290
57447.39800	0.8	312	291
57447.39856	0.8	252	281
57447.39912	0.8	531	295
57447.39968	0.8	285	280
57447.40024	0.8	450	392
57447.40192	0.8	703	361
57447.40248	0.8	1792	315
57447.40304	0.8	2010	346
57447.40359	0.8	4090	335	0.8	0.9
57447.40415	0.8	6860	326	0.8	0.5
57447.40471	0.8	10533	393	2.8	0.3
57447.40527	0.8	13288	368	2.0	0.2
57447.40583	0.8	15963	397	1.2	0.2
57447.40639	0.8	18081	419	1.4	0.2
57447.40695	0.8	16563	378	0.5	0.2
57447.40751	0.8	16816	404	0.9	0.2
57447.40807	0.8	13745	355	-1.0	0.2
57447.40862	0.8	12180	869	-1.2	0.8
57447.40974	0.8	3272	581
57447.41030	0.8	4674	327	0.9	0.8
57447.41086	0.8	3462	300	1.5	1.1
57447.41142	0.8	1859	335
57447.41198	0.8	2085	344
57447.41254	0.8	1719	306
57447.41310	0.8	1699	326
57447.41366	0.8	1220	279
57447.41421	0.8	1355	327
57447.41477	0.8	1337	292
57447.41590	2.4	1117	199
57447.41758	2.4	1399	347
57447.41926	2.4	677	176
57447.42094	2.4	806	167
57447.42261	2.4	1225	180
57447.42429	2.4	1170	205
57447.42597	2.4	544	252
57447.42765	2.4	1409	187
57447.42932	2.4	1155	197	-0.9	1.7
57447.43100	2.4	1079	188
57447.43268	2.4	763	258
57447.43436	2.4	1201	253
57447.43604	2.4	645	188
57447.43772	2.4	614	202
57447.43939	2.4	1154	229
57447.44107	2.4	275	373
57447.44275	2.4	558	260
57447.44443	2.4	457	214
57447.44611	2.4	400	195
57447.44778	2.4	352	212
57447.44946	2.4	195	468
57447.45114	2.4	425	175
57447.45282	2.4	384	192
57447.45450	2.4	757	201
57447.45617	2.4	333	178
57447.45785	2.4	770	520
57447.45953	2.4	142	184
57447.46121	2.4	420	210
57447.46289	2.4	25	173
57447.46456	2.4	420	192
57447.46624	2.4	241	279
57447.46792	2.4	89	148

Notes: a) $S_{15.5GHz}$ is the peak pixel values at the location of SS Cyg. b) σ_S is the RMS noise. c) The spectral index values having uncertainties less than two are noted here.